DOI: 10.13009/EUCASS2022-6103
9TH EUROPEAN CONFERENCE FOR AERONAUTICS AND SPACE SCIENCES (EUCASS)

Thermal management principal analysis of hybrid-electric aircraft with turboelectric propulsion using distributed propulsors

J. van Muijden and V.J.E. Aalbers**
**Royal Netherlands Aerospace Centre (NLR)*
Anthony Fokkerweg 2, 1059 CM Amsterdam, The Netherlands
Jaap.van.Muijden@nlr.nl
Jos.Aalbers@nlr.nl

Abstract
A proposed thermal analysis method is outlined with the specific purpose of performing thermal management principal analysis of innovative aircraft configurations using hybrid-electric propulsion. The focus is on the specific architecture and lay-out of a conservative Small-to-Medium Range aircraft configuration, although it can be adjusted to fit other configurations as well. Consecutive steps in the process and initial results are presented. Progress on electrical component efficiencies and advanced cooling technology is required to achieve hybrid-electric propulsion with acceptable weight penalties for the thermal management system. Also, an outlook to the follow-up phase aiming for enhanced details and accuracy is described.

1. Introduction

The societal call for environmentally friendly aircraft has put significant emphasis on the study of disruptive greener aircraft concepts and viable alternatives for gas turbine powered aircraft [1][2]. One of the options, hybrid-electric propulsion, is currently being investigated for its merits to reduce fuel consumption within the European project IMOTHEP, an acronym for “Investigation and Maturation Of Technologies for Hybrid-Electric Propulsion” [3]. The benefits of such architectures, however, may be counteracted by the thermal management challenges involved in electrification of propulsion drive trains [4].
In the present study, a generic approach is pursued to identify the specific thermal challenges involved and to provide an analysis methodology for the impact assessment of the thermal impact on overall aircraft design. As there is an urgent need for the inclusion of the expected impact of the necessary thermal management weight penalty already early in the preliminary design stages of new, innovative configurations, the thermal management principal analysis needs to be based on rather coarse configuration and propulsion assumptions derived from Top Level Aircraft Requirements (TLARs) without too much detailed knowledge of the geometry and (sub-)systems. As such, the thermal management principal analysis approach needs to be based on straightforward yet robust engineering concepts and allow for updates of detailed knowledge during evolution of the design.
Within the sketched framework, we limit ourselves to study the thermal management of turboelectric propulsion drive trains for a conservative Short-to-Medium Range aircraft configuration (SMR-con) of size comparable to an Airbus A320neo, based on the notion that the experience gained and the approach used in the problem set-up could be applied to other architectures and aircraft types as well (note that within IMOTHEP four different aircraft concepts are being studied). A specific characteristic of turboelectric propulsion using distributed propulsors is the significant increase of the number of non-negligible heat sources within the aircraft while the cooling of all those distributed heat sources is not a priori trivial.
The thermal management principal analysis is intended to provide useful engineering information on the following aspects early in the design stages of hybrid-electric configurations:
1. a first impression of the expected heat loads and the distribution of heat loads over the aircraft;
2. the capability to maintain component and coolant temperatures within preferred ranges;
3. to identify if and what additional measures should be taken to match the design objectives;
4. to compare alternative options with legacy cooling approaches.

DOI: 10.13009/EUCASS2022-6103

2. SMR-con configuration

Within IMOTHEP, the baseline electrical architecture of the power train for the SMR-con has been borrowed from the underlying DRAGON configuration as depicted in Figure 1. The DRAGON configuration (Distributed fans Research Aircraft with electric Generators by ONERA) is a turboelectric concept with distributed electric propulsion (DEP) using many identical electrical motors driving the same number of ducted fans. The propulsion drive train is based on two gas turbines located at the rear of the fuselage with the sole purpose of driving four generators to produce the energy needed for the propulsion of the aircraft. Propulsion is done by the electric motors in separate ducts underneath the wing near the trailing edge. The DRAGON configuration has improved propulsive efficiency due to DEP and boundary layer ingestion (BLI). Its performance is depending on the efficiency of the electrical machines employed.

Figure 1: Artist impression of DRAGON configuration (courtesy: ONERA[5])

The details of the electrical lay-out of the envisaged architecture for the DRAGON configuration have been published by Schmollgruber [6]. Figure 2 shows the main lines of thought for this particular architecture, as they are also relevant to the power distribution and failure modes of the drive train of the SMR-con which follows a similar set-up.

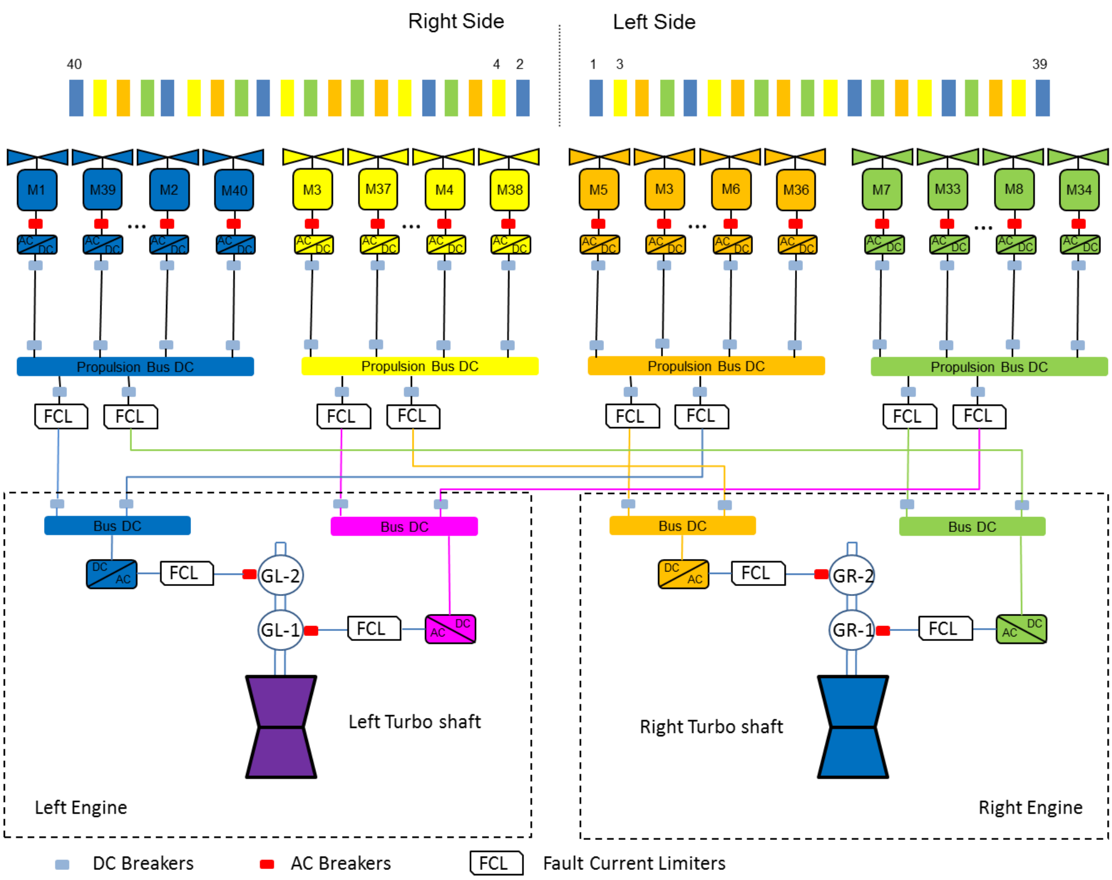

Figure 2: Electrical architecture set-up of the DRAGON configuration (example with 40 motors)

DOI: 10.13009/EUCASS2022-6103

The architecture is divided in a left and a right side of the aircraft. The two turboshafts each drive two electrical generators. Each generator has a different color and feeds an electric bus of the same color. The fault current limiters (FCL) are included as security devices to keep most of the electrical network functioning in case of a short circuit event. Furthermore, in order to reduce the impact of failure, the four electrical DC-buses each feed two propulsion DC-buses that transfer power to the inverters and motors. By smart alternating connection of inverters and motors to the available propulsive buses, there is always propulsive power on each side of the aircraft. Even in the case of severe failures, this set-up provides the best chance of evenly distributed propulsive power over the wing.
In contrast to the DRAGON configuration of Figure 1, the SMR-con has only 24 motors. The mission profile for the SMR-con is divided in the following main segments: take-off and initial climb, climb, cruise, and descent. Cruising is done at a Mach number of 0.78 at about 11 km altitude. The most critical flight segments in terms of thermal loads are those with full or almost full power, i.e. take-off and initial climb as well as climb. When the aircraft reaches top-of-climb, it has been subjected to a lengthy period (about half an hour) of almost maximum power and heat rejection which has put maximum stress on the thermal management system. Furthermore, it is anticipated that ground idle conditions, especially on a hot day, and flight idle conditions may pose risks for cooling capability as the air speed is limited or even absent. For the principal analysis, the take-off and top-of-climb conditions are primarily selected as interesting cases. One additional very important aspect for thermal management is the ambient atmospheric condition on the ground. On a very cold (-40 C or ISA-55, ISA stands for International Standard Atmosphere [7]) or a very hot day (55 C, or ISA+40), the ability to reject heat into the ambient environment is completely different. Thus, deviations from standard atmosphere must be included in the assessment of thermal management effectiveness.
In a full-functioning architecture as depicted in Figure 2, the heat loads are symmetrical in nature. This finding follows the basic rule that similar components deliver equal contributions to the demanded overall propulsive power, have similar characteristics in terms of efficiency, losses, and thermal limitations. For failure cases, however, there may no longer be a valid basis for symmetry considerations between left- and right-hand side of the aircraft. It depends on the power management system how the failure case is handled, e.g. by redistributing the available power using the remaining margins of the still functioning components.
For the sake of the current principal analysis, we assume that the power redistribution on components can still be estimated using the assumptions as shown in Table 1 and Table 2. It should be noted that the failures have a downstream as well as an upstream effect. Downstream is defined here as the power distribution direction from engine to motor through the chain of components (see Figure 2), and upstream is the other way around. In the downstream view, there is no power going further downstream if a component fails and thus the dependent components fail too (the natural logical consequence). In the upstream view, it is assumed that no power is lost to feed functioning components that are only feeding failed components. Instead, it is assumed that power redistribution to the remaining functioning components takes place to make the best use of available power. Confirmation of these assumptions needs to be validated at a later stage against the implemented power management system control laws.

Table 1: Failure cases and impact on power distribution (downstream view)

Failure	**Assumed impact**
1 motor out	Other motors work harder
1 inverter out	Connected motor out
1 propulsion bus out	The connected 6 motors and inverters out
1 distribution bus out	All propulsion buses still powered
1 rectifier out	Connected propulsion bus out
1 generator out	Dependent propulsion bus and rectifier out
1 engine out	Two dependent generators out

DOI: 10.13009/EUCASS2022-6103

Table 2: Failure cases and impact on power distribution (upstream view)

Failure	Assumed impact
1 motor out	Connected inverter out
1 propulsion bus out	Redistribution of power demand
1 distribution bus out	Connected generator and rectifier out

3. Thermal analysis

3.1 Outline of methodology

For the purpose of a principal thermal analysis, the simulation is based on a nodal network representing aircraft compartments that have a temperature and associated thermal properties like mass and specific heat. This approach avoids the time-consuming high-fidelity solution of partial differential equations for fluid flow including heat transfer or partial differential equations for conduction in solid bodies. High-fidelity simulations are only useful when the geometry and material properties are already known in substantial detail. This is usually not the case in a (preliminary) design iteration mainly based on TLARs. In that stage of engineering, the details are usually far from converged and obtaining a thermal analysis is more efficient on the basis of an approximate nodal model using lumping of mass into a limited number of nodes. In a nodal network, thermal paths to other compartments need to be identified. Compartments can be large or small, depending on the required accuracy and available details. For a principal analysis, large compartments are sufficient to get an impression on heat fluxes and resulting temperatures. In this respect, large means entire bays like avionics bay, flight deck, or cabin. For a more detailed design including sizing of heat exchangers, cooling systems and the like, there is a need for more detailed systems architecture and precise heat paths. The basis for a higher accuracy of modeling is formed by a global system architecture including subsystems. It might be needed to subdivide compartments into multiple smaller components.
The equations for the dynamic change of nodal temperatures in compartments take the following straightforward form[8][9]:

$$\boldsymbol{C}\frac{\boldsymbol{dT}}{\boldsymbol{dt}} = \boldsymbol{P} + \sum \boldsymbol{Q_{in}} - \sum \boldsymbol{Q_{out}}. \tag{1}$$

Here, C denotes the heat capacity of the node which is equal to the nodal mass times the specific heat of the material, T is the temperature of the node, and t is the time. On the righthand side, P denotes the heat production in the node itself – for example by combustion processes - and furthermore summation is done over heat fluxes Q going into and out of the node. Heat fluxes could be due to convection, radiation or conduction. The summation must include all applicable modes of heat transfer for a specific node. The heat flux is expressed as

$$\boldsymbol{Q} = \boldsymbol{qA}, \tag{2}$$

with q the heat flux per unit area and A a characteristic heat exchange area. In a most general fashion, the heat flux per unit area between two nodes can be expressed as

$$\boldsymbol{q} = \boldsymbol{h}(\boldsymbol{T_2} - \boldsymbol{T_1}), \tag{3}$$

where h is the heat transfer coefficient. Using this formulation, the heat flux automatically becomes positive or negative between two nodes in the nodal network, depending on the temperature difference. The summation over heat fluxes in and out of the node then simply adds up to a single summation over all heat fluxes defined for the node at hand, whether positive or negative. Of course, if multiple modes of heat transfer take place, the heat flux of each mode should be included in the summation.
For practical application of the outlined methodology, the following items are now key to the performance of the nodal approach: input data for thrust and Mach number per point in the mission profile, connections between compartments; assessment of the heat loads generated inside compartments; heat exchange via (sub-)systems; and estimates of heat transfer coefficients for the three heat transfer modes of conduction, convection and radiation. For the assessment of heat loads generated inside compartments, use is made of assumed efficiencies of electrical or other components in

DOI: 10.13009/EUCASS2022-6103

case no other information is available. In Table 3, the currently used assumed efficiencies for several components are given. These efficiencies and the results depending on them are easily updated in case better numerical values become available.

Table 3: Assumed efficiencies of main components

Component	Efficiency
Motor	0.98
Inverter	0.98
Electric bus	0.99
Cabling	1.00
Rectifier	0.98
Generator	0.95
Engine	0.46

3.2 Reduced thermal model

A reduced thermal model (RTM) of the SMR-con is based on the conceptual usage of main compartments in which equipment like avionics and other (sub-)systems or passengers and crew reside. The RTM of the SMR-con can be expressed in Cartesian form as shown in Figure 3.

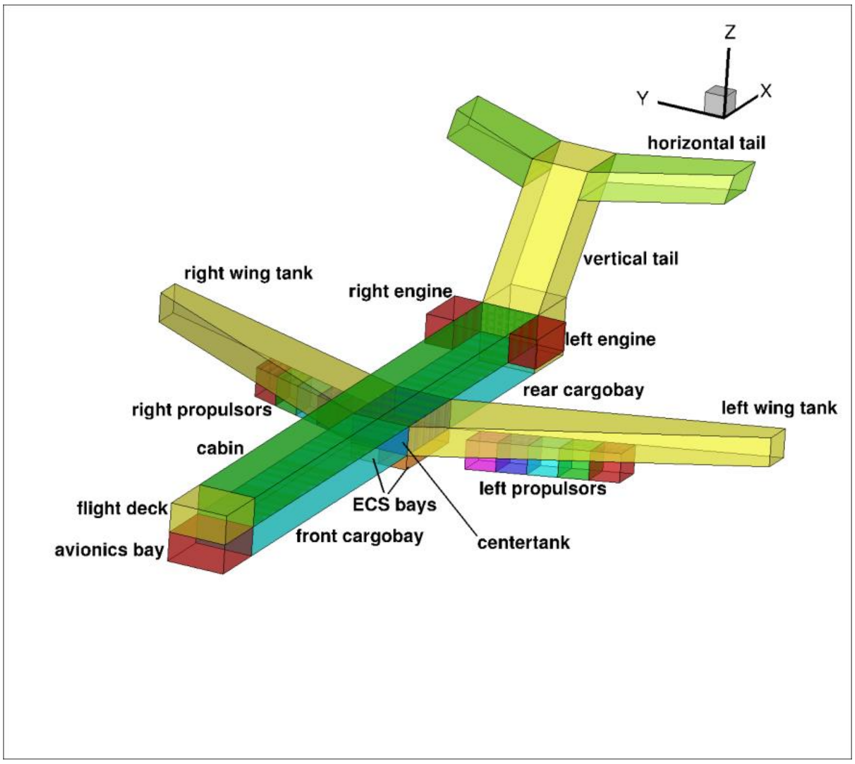

Figure 3: Conceptual representation of reduced thermal model (RTM) of SMR-con, based on main compartments.

Here, the compartments are roughly identified as prisms, and the main compartments that need to be in the model have been included (and a few others too in order to make the complete model at least look like an aircraft). The model is

DOI: 10.13009/EUCASS2022-6103

not yet to scale and not conformal to the actual aircraft shape and the number of propulsors is not fully elaborated, but scaling to actual size can be included to a high degree of accuracy when available information on its dimensions has been processed. If necessary also the shape could be improved based on actual outer mould line geometry, although that step does not really add value to the interpretation. The model provides insight into connected bays and extent of external surfaces and can be used to support the assessment of compartment heat loads and their interactions, e.g. for area estimations. As an initial step, the RTM is sufficient to support thermal calculations provided it is brought to actual scale, but in a follow-up step we need to couple the bays with the detailed interaction scheme of (sub-)systems.

3.3 Compartment heat loads

Engine nacelle

In each engine nacelle, one engine, two generators and two rectifiers are placed. The heat loads of these components find their way into the nacelle although some heat of the engine is directly expelled through the exhaust. The engine powers, losses and efficiencies for a conventional aircraft gas turbine are most conveniently explained by the indicative schematic power representation of Figure 4. The schematic representation shows five stadia and these will be outlined below while using selected literature [10][11][12] to arrive at appropriate expressions.

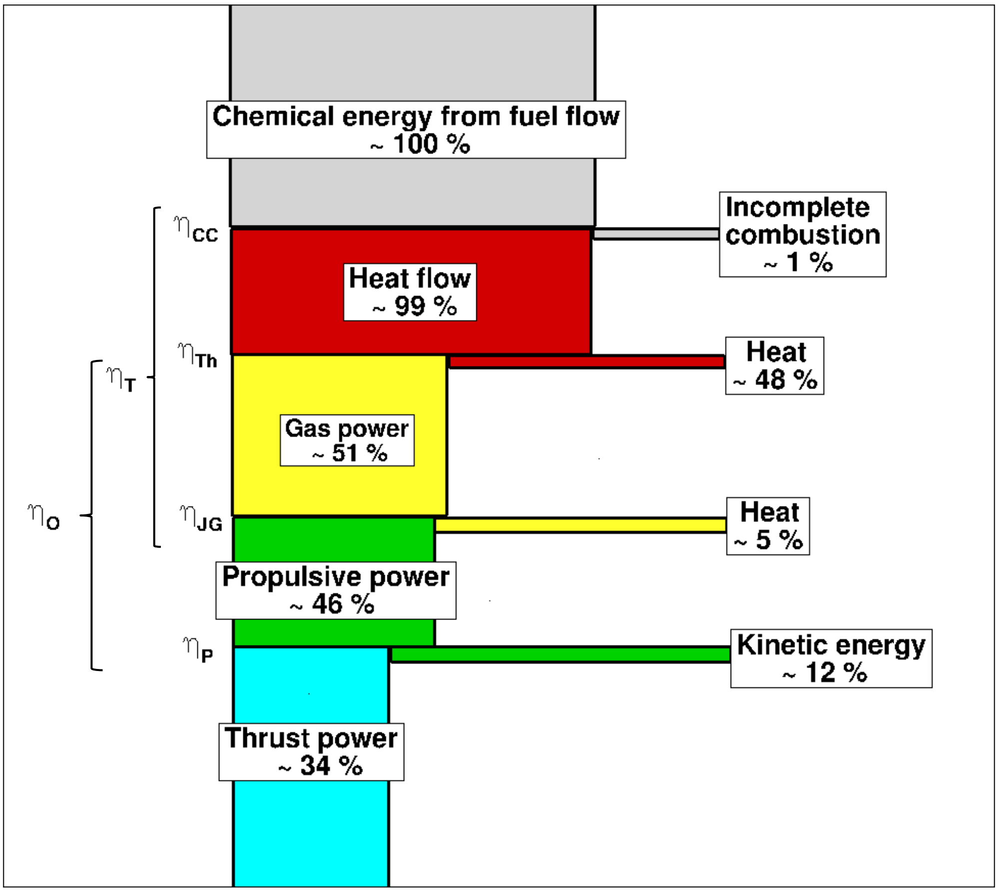

Figure 4: Schematic representation of powers, losses and efficiencies in an aircraft gas turbine engine (percentage numbers indicative only, based on 1980-technology status)

In Figure 4, the total energy inflow per unit time is entering the gas turbine in the form of fuel flow and it is indicated on purpose by approximately 100 percent chemical combustion power content as the fuel may be used as coolant and therefore may have variable inflow temperature already. The chemical combustion power based on the fuel flow is written as the product of fuel mass flow and the lower heating value of the fuel:

$$Q_f = \dot{m}_f \, LHV. \tag{4}$$

Due to incomplete combustion, about 1 percent of the heating power is lost in the transition to the second stadium. The efficiency in the conversion from chemical power to heat flow is denoted as the combustion chamber efficiency. It is defined as

DOI: 10.13009/EUCASS2022-6103

$$\boldsymbol{\eta_{CC} = Q_{CC}/Q_f,} \tag{5}$$

where the heat absorbed by the gas flow through the engine core Q_{CC} is defined in terms of the total enthalpy increase of the gas (subscript g referring to gas, c_{pg} is the specific heat of the gas at constant pressure):

$$\boldsymbol{Q_{CC} = c_{pg}\, \dot{m}_g\ \Delta T_{tg}.} \tag{6}$$

In the second stadium, a large part of the heat flow is lost in radiation, conduction and convection due to the very high temperature of the gas flow, heating up the engine itself and its direct surroundings. The power part lost in heating of the environment is no longer available for jet generation and thus reduces the available gas power. The efficiency in this step is the thermodynamic efficiency, defined as

$$\boldsymbol{\eta_{Th} = P_g/Q_{CC}.} \tag{7}$$

A common expression for gas power in terms of achieved total pressure and temperature in the engine core flow is (subscript 0 denoting free stream conditions, p is the pressure, v is the velocity, γ is the ratio of specific heats)

$$\boldsymbol{P_g = c_{pg}\dot{m}_g T_{tg}\left[1 - \left(\frac{p_0}{p_{tg}}\right)^{\frac{\gamma_g - 1}{\gamma_g}}\right] - \frac{1}{2}\dot{m}_g v_0^2}\ . \tag{8}$$

The gas flow can be expanded to generate a jet, and the conversion of gas power into propulsive power is suffering from an additional heat loss of about 5 percent. The efficiency involved in this transfer is the jet generation efficiency

$$\boldsymbol{\eta_{JG} = P_P/P_g,} \tag{9}$$

with the propulsive power defined as the actual increase of the kinetic energy per unit time of the gas stream (subscript j denoting jet)

$$\boldsymbol{P_P = \frac{1}{2}\ \dot{m}_g\left(v_j^2 - v_0^2\right).} \tag{10}$$

The thermal efficiency commonly used in gas turbines is defined as the efficiency of the conversion of the heat energy released by the fuel into kinetic energy in the jet stream and is the product of the combustion chamber efficiency, thermodynamic efficiency, and jet generation efficiency:

$$\boldsymbol{\eta_T = \eta_{CC}\, \eta_{Th}\, \eta_{JG}.} \tag{11}$$

Finally, the transition to the fifth stadium is the actual result of the generated propulsive power into forward motion of the aircraft, denoted as the thrust power, defined as

$$\boldsymbol{P_F = F\, v_0.} \tag{12}$$

Here, $\boldsymbol{F}$ denotes the thrust of the engine, which is defined as the difference between momentum at the jet exit and at freestream entrance conditions, supplemented with a pressure term on the jet nozzle with area A_j:

$$\mathbf{F} = \boldsymbol{(\dot{m}\, v)_j - (\dot{m}\, v)_0 + (p_j - p_0)A_j}\ . \tag{13}$$

Usually, the nozzle is designed to equalize the exhaust pressure and the ambient pressure, so that for an ideal nozzle the latter pressure term can be neglected. Furthermore, the fuel flow rate is in general much smaller than the air flow rate and is often ignored in the exhaust term. The propulsive efficiency compares how much work is done on the aircraft by supplying kinetic energy to the air and is defined as

$$\boldsymbol{\eta_P = P_F/\, P_P}\ . \tag{14}$$

The overall efficiency of the engine compares the work done on the aircraft to the energy given by the fuel and is the product of thermal efficiency and propulsive efficiency:

DOI: 10.13009/EUCASS2022-6103

$$\boldsymbol{\eta_O = \eta_T\, \eta_P\ .} \tag{15}$$

Using the equations above, an expression for the power lost into kinetic energy per unit time is

$$\boldsymbol{P_{kin} = P_P - P_F = \frac{1}{2}\, \dot{m}(v_j - v_0\,)^2.} \tag{16}$$

As is shown in Figure 4, most of the heat produced by the engine stays in the engine nacelle or engine itself and needs to find its way out through the engine cooling system or passive heat transfer. In view of available information, the data for the heat produced by the engine is currently limited to an assumed overall efficiency. In the next phase, feedback from the detailed engine design work is envisaged to allow for more precise engine heat source estimates.

ECS bay thermal loads

Thermal loads that need to be controlled by the environmental control system (ECS) are basically the heat production in the cabin, flight deck, and avionics bay. Cooling of the cabin, flight deck and avionics bays is done by the ECS system using bleed air from the gas turbine in a legacy setting, or compressed air from an electrically driven air compressor in a modern aircraft architecture. The ECS-system is located in the ECS bay. There may be more than one ECS pack in an aircraft, each in its own bay. A common location of the ECS bays is in the wing-fuselage fairing underneath the central wing box. Its functions are to provide air supply, thermal control and cabin pressurization. The ECS-system consists of a compressor, turbine and water separator and potentially also some heat exchangers. Conventional architectures make use of a Brayton cycle to cool compressed air to appropriate temperatures and provide dehumidification for its diverse clients [13].

Cabin thermal loads

Heat production inside the cabin occurs by the maximum number of seated passengers and a few working crew members. Fanger [14] developed an initial basic theory of human thermal regulation and perception of the cabin environment and brought it together in a heat balance equation of the human body. It assumes that the human body behaves as a single node with a single temperature state. His equation, despite the basic modelling involved, has been adopted as a standard (ISO 7730 [15]) for the prediction of mean votes and percentage of dissatisfied people within a specified thermal environment. Distinction is made between sensible and latent heat loss. Sensible heat loss is related to the “dry” physical processes of conduction, convection and radiation. Latent heat loss is related to heat loss due to exhaled moisture in the respiratory air or by evaporation of sweat. More detailed and more accurate thermoregulation models of increasing complexity, using multiple body parts and layers as nodes, have been developed by e.g. Stolwijk [16], Tanabe [17] and Fiala [18]. The main take-away from all these theories for the current thermal considerations is the heat production per average occupant, expressed in metabolic equivalent of task (met) units (1 met = 58.2 W/m^2). The metabolic rate of the human body depends on activity: for seated passengers doing light activities it will not exceed $met = 1.2$. The somewhat higher metabolic rate ($met = 1.6$) of the few crew members can be ignored on the overall metabolic heat production. Stolwijk [16], Tanabe [17] and Fiala [18] take an average human to close their balances and assume a DuBois body surface area of about 1.9 m^2. Using these data, the metabolic heat production by occupants in an aircraft cabin due to their metabolism is expressed as

$$\boldsymbol{M = 58.2\ \#people\ A_{Du}\ met.} \tag{17}$$

Here, M denotes the metabolic heat production by occupants, $\#people$ is the number of people in the cabin, and A_{Du} denotes the DuBois body surface area. In this way, we do not distinguish between sensible and latent heat loss any more, but simply put the entire internal metabolic heat production as a heat source term into the cabin. In doing so, it is assumed that the power needed for moisture extraction from the cabin air is now already included in the overly rated cooling power for the sensible heat loss. This approach is sufficiently accurate for the current purpose. For an A320neo-sized aircraft with maximum capacity in a single class lay-out having 193 people in the cabin, this amounts to a heat source of $M = 25.6\ kW$. This amount of heat needs to be controlled by cooling. Furthermore, in order to keep the occupants satisfied the temperature in the cabin should be kept constant at about 24 degrees Celsius [19].

Apart from the human metabolism, other heat sources may be present in the cabin, e.g. in-flight entertainment systems, galley equipment, etc. The heat production from these additional components can be calculated if data are available on equipment power, efficiency, and operational duration. Galley equipment is more often used in short-duration intermittent operation modes and may only contribute temporarily to the overall cabin heat loads.

Flight deck thermal loads

The number of people on the flight deck is too low to produce a relevant amount of heat. Actually, the flight deck may in general require heating to maintain a comfortable working environment, despite the equipment located in the cockpit.

DOI: 10.13009/EUCASS2022-6103

Avionics bay thermal loads
The installed overall power of the combined avionics systems and assumed average efficiency deliver an estimate of the required cooling power.

Fuel tank thermal loads
Fuel tanks are located in the wing box and fuselage centreline and will lose heat at altitude through the wing surface. Due to the large mass of fuel on board and the fact that it is consumed during flight, it forms a very useful heat sink before combustion, thereby expelling part of the heat through the engine exhaust. In some cases, fuel can be recirculated after being used as coolant, thus slightly increasing the overall temperature of the fuel in the tanks. As long as the maximum acceptable fuel temperature is controlled, the fuel mass provides a significant heat sink. Common use of fuel as coolant is in fuel-oil heat exchangers, cooling down the engine oil or the hydraulic oil.

Cargo bays thermal loads
Cargo bays do not play a direct active role in the thermal balance of the aircraft, although the air contained in the cargo bays may serve as heat sink. In general, cargo bays are pressurized but not temperature controlled unless there is a specific reason to do so. Cargo bays take up heat through the floor separating the bays from the cabin. Also, aircraft system tubing through the cargo bay may deliver some heat. In general, the cargo bay will remain cool at altitude due to the large outer surface. In both cases, i.e. temperature controlled and uncontrolled, the cargo bays can be used to dump excessive heat from other systems.

3.4 Thermal control requirements and TMS weight penalty

Drive train components, especially the electrical ones, have a preferred temperature range for optimal performance during normal operations. Too low or too high temperatures of components will lead to damage or increased chances of failure of those components. Based on literature, an initial set of temperatures limitations has been compiled for components, for coolants, and for fuel. These ranges function as important boundary conditions on the operational capabilities of the thermal management system.
Giving an estimate for thermal management system volume and weight, and thus being able to provide an estimate of the impact of the TMS on the overall configuration design, is not an easy task. For a start, a design estimate for lumped cooling system mass penalty has been identified, but this provides only a very crude approach. The value used to arrive at a weight estimate is based on a power-specific mass penalty of 680 W/kg. A remark accompanying this number is that it holds only for conventional architectures. In view of overall heat rejection originating out of the calculation method (see Chapter 4), this would imply an initial TMS weight penalty estimate of more than 4 tonnes. Numbers like this have led to the conclusion that individual efficiencies of components need to be improved and that more detailed assessment of designs is mandatory.
Validation and further elaboration on this number is needed in the follow-up phases of thermal design. A somewhat more sophisticated approach, based on preliminary heat exchanger sizing, is outlined in Wolff [20]. Here, weight and volume estimates of heat exchangers (HX) are based on considerations for HX-geometry, characteristics like porosity, and engineering correlations. In the next phase of TMS design, outcomes of dimensioning from partners involved in component studies can be compared to results given by such methods.

4. Results

Three cases are considered here for which power derivations and heat rejection data have been generated. Case 1 is for a full-power take-off condition at a Mach number of 0.23 in an ISA+18 temperature environment for a full-functional drive train. The input power and heat dissipation of components are shown in Figure 5 and Figure 6. This condition requires a total fuel flow of approximately 1.3 kg/s equaling a heat power of 57.6 MW. Of this power, only about 40 percent is effectively used for propulsion purposes. Apart from the engines, where 54 percent of the fuel flow energy is lost in heat, about 3.3 MW or 15 percent of the installed propulsive power is dissipated as heat in electrical components. Case 2 is selected at top-of-climb, just after power reduction for cruise (otherwise it would not have been much different from the take-off case), at an altitude of 11 km and a Mach number of 0.78 in an ISA+18 temperature environment for a full-functional drive train. The results are shown in Figure 7 and Figure 8. Case 3 is equal to case 2, however with an assumed failure in one of the propulsion buses. The results are shown in Figure 9 and Figure 10. In this failure case, it has been assumed that the needed overall power is still delivered by the remaining functioning components and power redistribution has taken place in accordance with the description and assumptions made in Chapter 2. In all examples above, the lower heating value (LHV) of fuel is given by 43.15 MJ/kg, representative for Jet A-1 fuel. This value has been used to calculate the fuel flow rate that is needed to provide the requested power. It should further be noted that it has been assumed that the engines themselves do not provide propulsive power.

DOI: 10.13009/EUCASS2022-6103

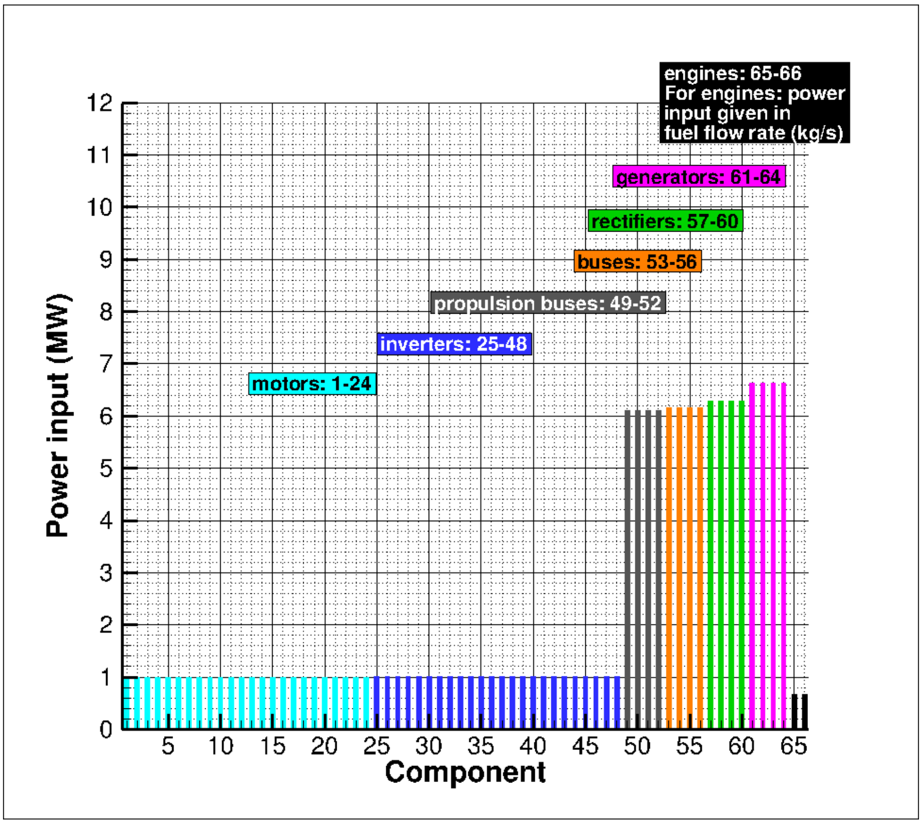

Figure 5: Power input to fully operational drive train components at ISA+18 temperature conditions for zero altitude and Mach number of 0.23.

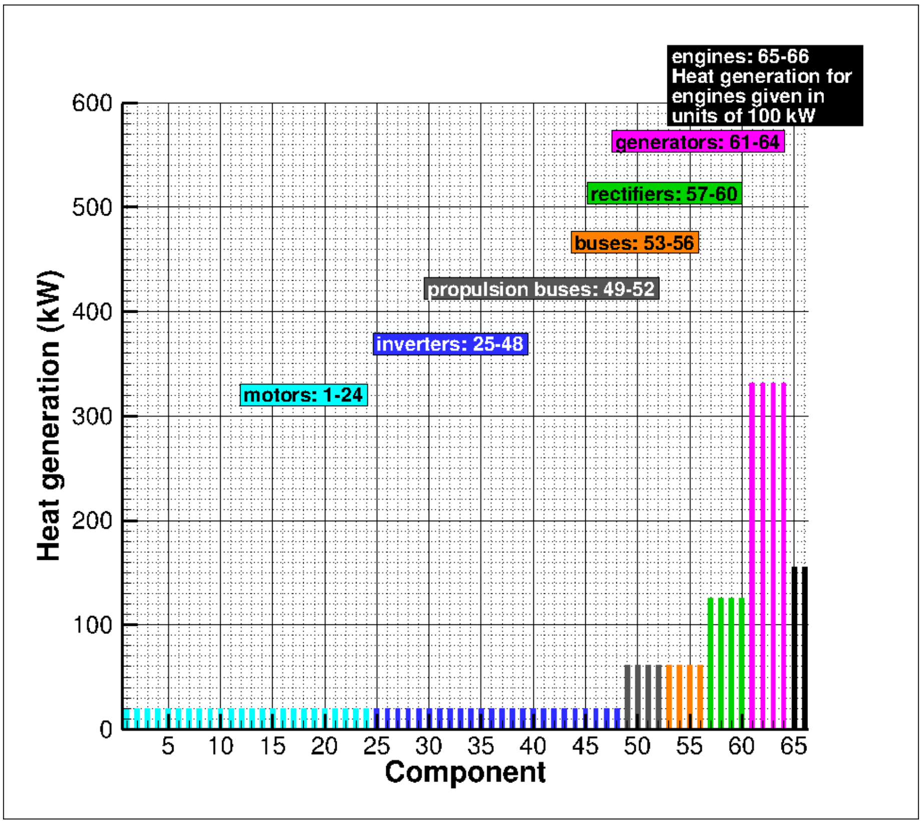

Figure 6: Heat losses in fully operational drive train components at ISA+18 temperature conditions for zero altitude and Mach number of 0.23.

DOI: 10.13009/EUCASS2022-6103

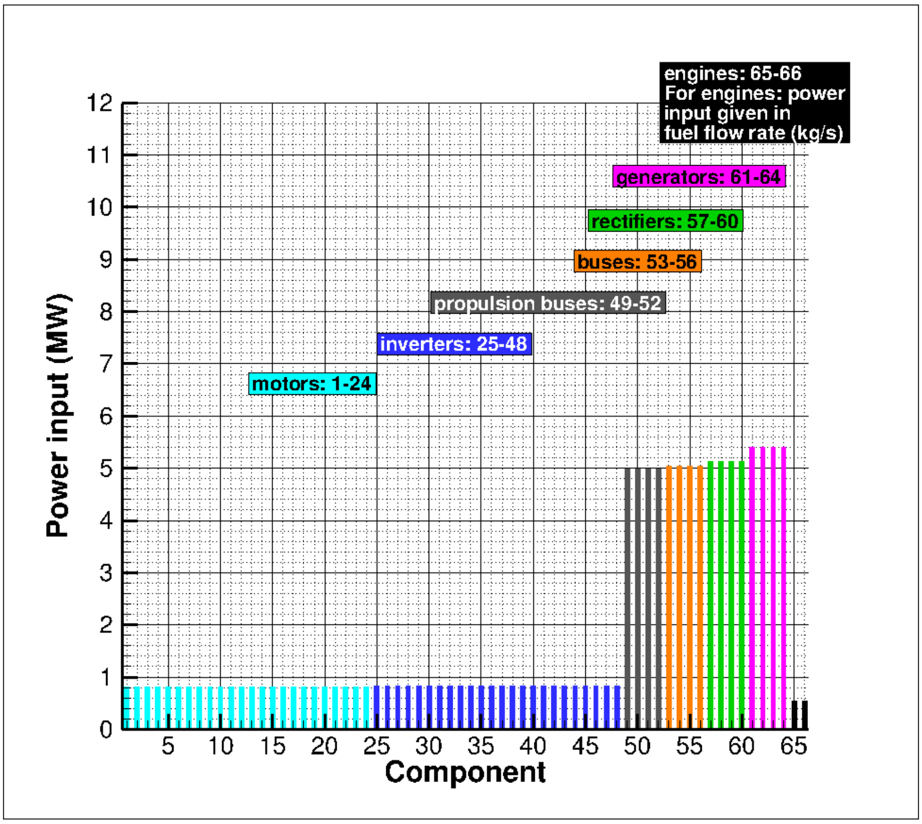

Figure 7: Power input to fully operational drive train components at ISA+18 temperature conditions for 11 km altitude and Mach number of 0.78.

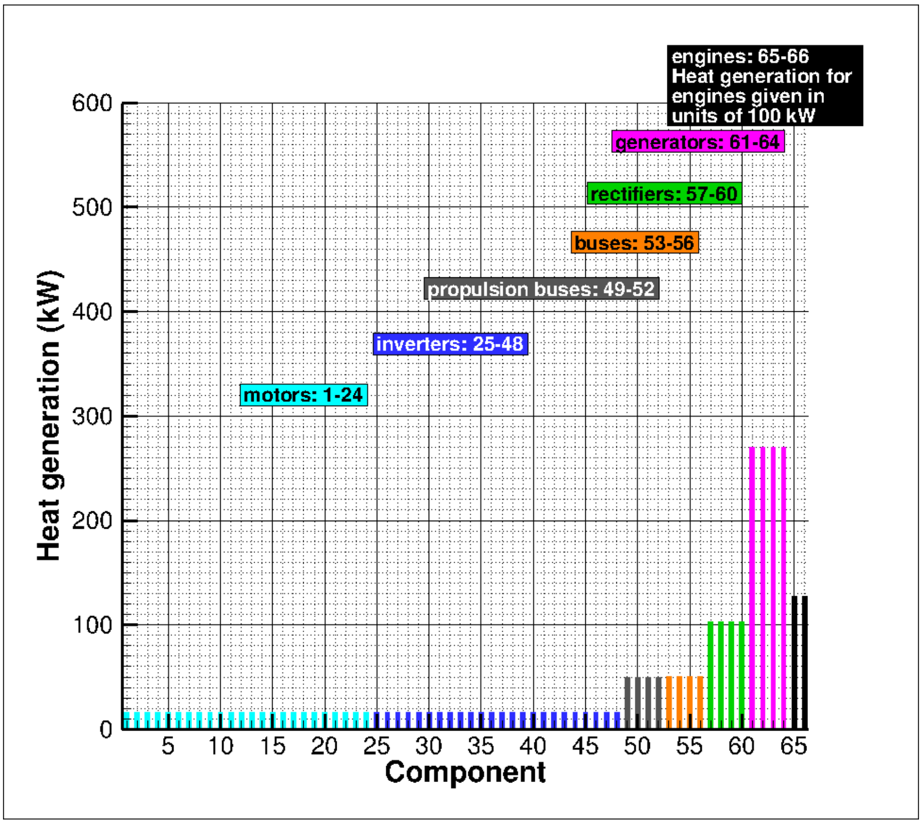

Figure 8: Heat losses in fully operational drive train components at ISA+18 temperature conditions for 11 km altitude and Mach number of 0.78.

DOI: 10.13009/EUCASS2022-6103

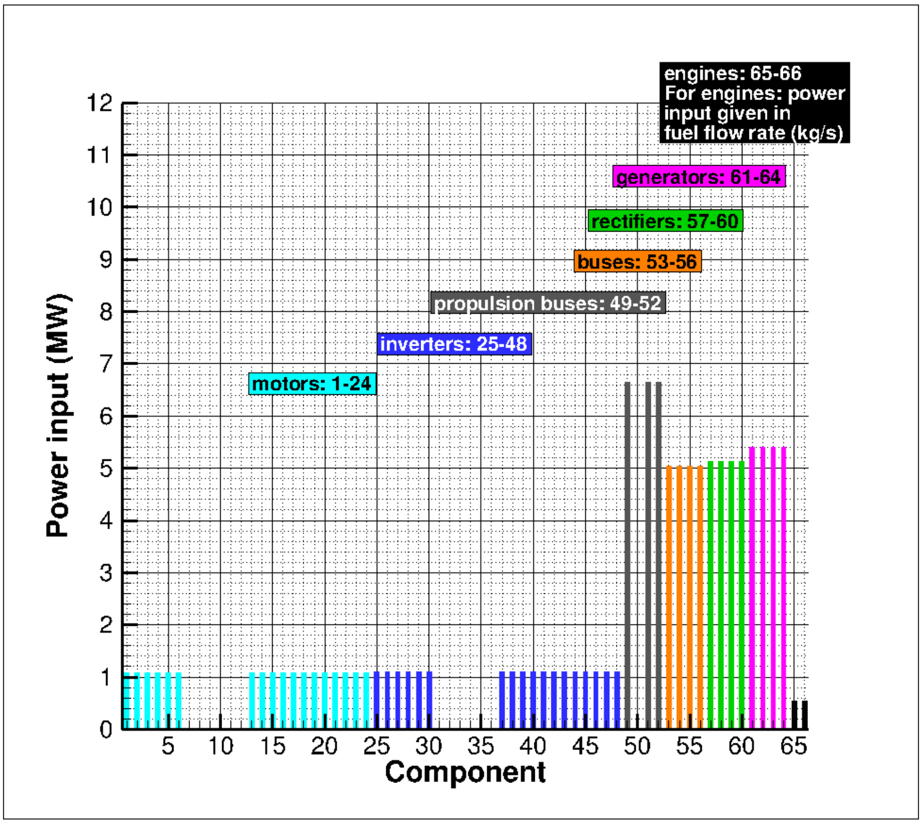

Figure 9: Power input to drive train components at ISA+18 temperature conditions for 11 km altitude and Mach number of 0.78; failure case in one of the propulsion buses.

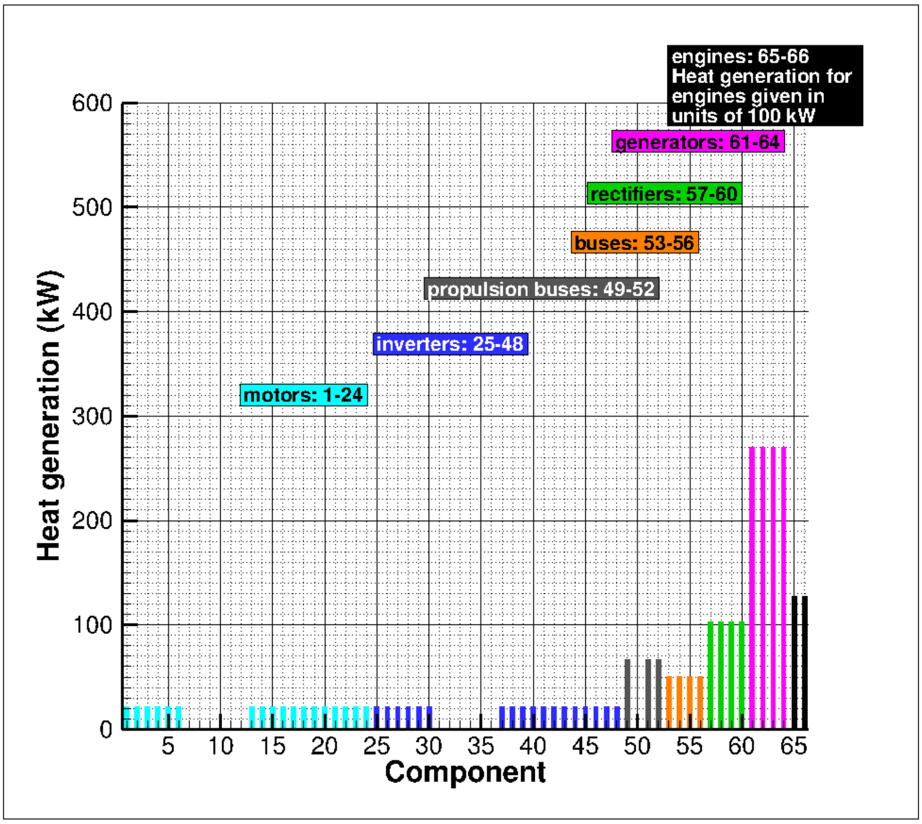

Figure 10: Heat losses in drive train components at ISA+18 temperature conditions for 11 km altitude and Mach number of 0.78; failure case in one of the propulsion buses.

DOI: 10.13009/EUCASS2022-6103

5. Outlook to follow-up phase

In the next phase of the thermal management activities within IMOTHEP, several items are foreseen to be brought in a more accurate connection to each other, based on the building blocks presented in this paper. For the sake of focus and budget efficiency, this involves a split-up of responsibilities over (sub-)systems between partners working in the thermal management task. The interaction between (sub-)systems, the link to the compartments in the RTM, values for heat transfer coefficients and areas, and educated volume and mass penalty calculations for the additional weight of the TMS are on the list of items. As far as the interaction of (sub-)systems is concerned, an interaction scheme has been devised to study the specific interactions anticipated for the SMR-con, see Figure 11 for the current status.

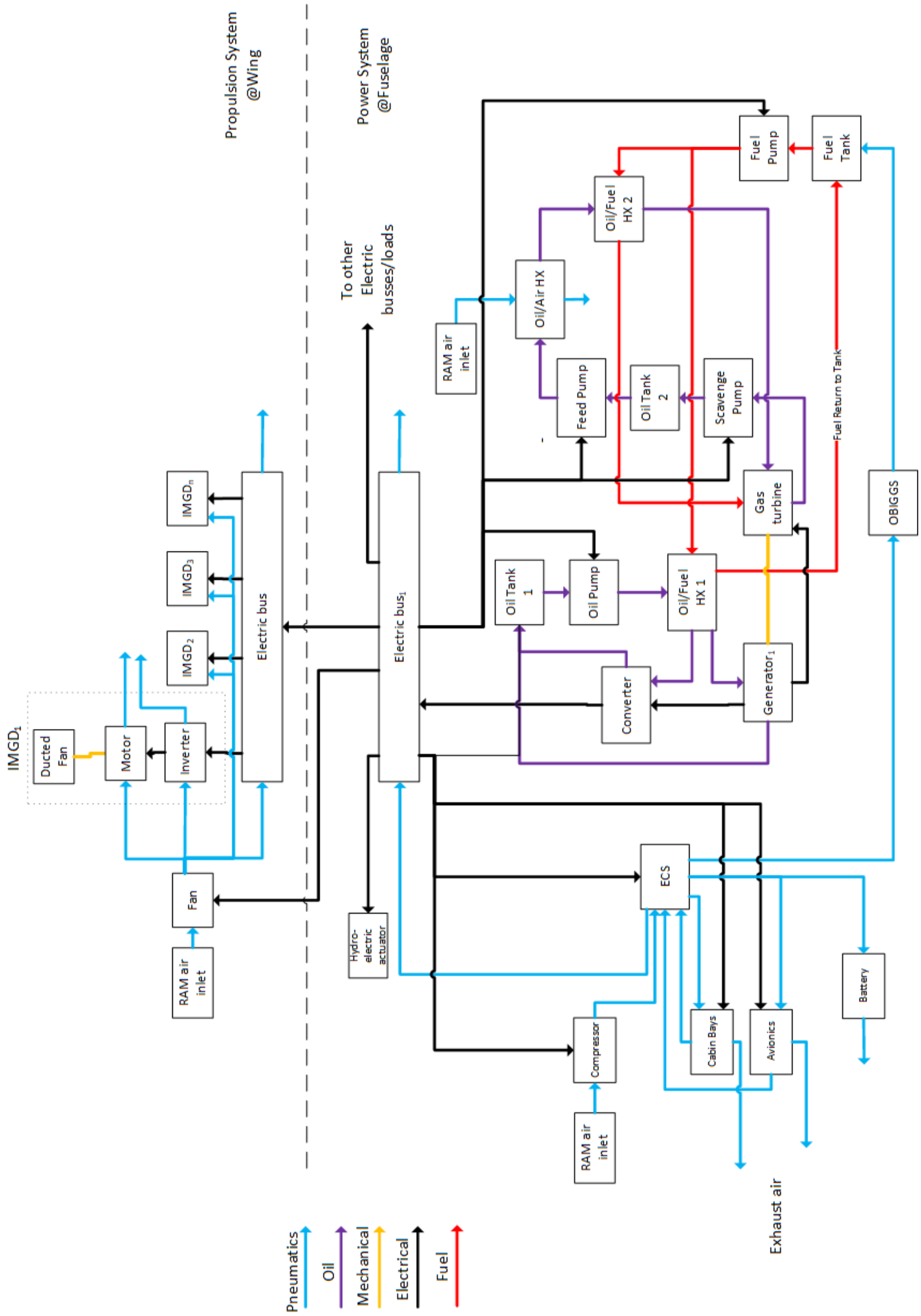

Figure 11: Schematic representation of interactions between pneumatic, hydraulic, mechanical, electrical and fuel systems for in-depth analysis of heat transfer.

DOI: 10.13009/EUCASS2022-6103

The gas turbine provides mechanical power via the power take-off shaft (PTO) to the generators connected to it. The generators provide electric power to the distribution and propulsion buses that eventually drives the motors of the propulsors. For this, fuel needs to be fed to the gas turbine. The fuel is also used as heat sink, so it flows through several fuel-oil heat exchangers (HX) before being burnt or being returned to the fuel tank. Fuel is moved by an electric fuel pump in this case. Engine oil is used to lubricate the gas turbine, it will significantly heat up during operation and needs to be cooled using an air-oil heat exchanger, fed by a ram air inlet, as well as a fuel-oil heat exchanger. Electrically driven oil pumps are used to feed the engine oil to its destination and to return it to the oil tank. The generator is cooled down with hydraulic oil from another oil tank by an oil pump that pushes the coolant through a fuel-oil heat exchanger to the generator, where it is sprayed on the coils. Also, the converter (rectifier) is cooled with the same coolant oil. This part concludes the fuel, pneumatic and mechanical power connections.

Then, there is the pneumatic system picking up ram air from outside for the ECS-system. The schedule shows where pressurized and thermally controlled air is going to from the ECS-system, assuming the ECS-system delivers cool air and pressurization to the cabin, flight deck, avionics bay, fuel tank, and other components like batteries and electric buses. The ECS-system is important for thermal control of components as well as thermal comfort and pressurization of the cabin and flight deck for passengers and crew.

Another branch of the pneumatic system is for propulsion purposes. The propulsor ducts take air in through the inlets and accelerate the air via a fan driven by a motor. The connection between motor and propulsor is once again a mechanical connection. The air through the propulsor ducts is also used for cooling of the motor and the power electronics.

Work in the next phase comprises more detailed system analysis for engine and its diverse heat exchangers, for the ECS, the fuel system, the propulsors, etc. Requirements and sizing for the cooling system components will need to be elaborated. Furthermore, the connection with the compartment-based RTM-model will be made in more detail by identifying where all the components are located and to what extent the heat loads become problematic locally.

6. Conclusions

Building blocks are presented that form the first level of an integrated thermal management system (TMS) set-up for a short-to-medium range aircraft in a conventional tube-and-wing layout (SMR-con), equipped with fuselage-mounted gas turbine engines for electricity generation and a large number of underwing electric propulsors for thrust generation. The drive train concept is borrowed from the DRAGON configuration and adjusted to match the currently foreseen 24 propulsors. The routine for power demands and heat generation calculates data for input powers and heat production in the drive train components, based on input values for component efficiencies, flight condition (Mach number and altitude), required thrust, and atmospheric deviations from standard atmosphere. Failure cases and the resulting asymmetrical thermal loads on drive train components can be handled too, although assumptions regarding power redistribution during component failures still need to be validated against actual power management implementations. Results for the heat production in components have been shown for selected conditions from the mission profile. The reduced thermal model (RTM) is intended to provide visualization options for the resulting temperature distribution in the configuration at any moment during the flight, following the distributed heat generation within compartments of the configuration, and to support assessment of data for the evaluation of heat exchange between compartments.

In the follow-up phase, it is intended to link more detailed analysis of (sub-)systems and their anticipated cooling implementations to the RTM and to improve the accuracy of compartment and component temperature predictions. For this purpose, a schedule for the overall aircraft system interactions has been devised for the SMR-con. The effort of project partners involved in the thermal work package has been split up over components to match their respective interests and to maximize budgetary efficiency. The contributions from different partners ultimately need to be combined into the next level of the integrated TMS. Also, weight and volume penalties for the TMS need to be elaborated to a higher level of accuracy.

Acknowledgment

The reported work has been performed within the framework of the IMOTHEP project. The authors acknowledge the valuable discussions with and contributions of IMOTHEP partners to this work as well as the funding received from the European Union Horizon 2020 programme under grant agreement No. 875006.

References

[1] Kim, J.H., K.S. Kwon, S. Roy, E. Garcia, and D. Mavris. 2018. Megawatt-class turboelectric distributed propulsion, power, and thermal systems for aircraft. AIAA paper 2018-2024.

DOI: 10.13009/EUCASS2022-6103

[2] Larkens, R. October 2020. A coupled propulsion and thermal management system for hybrid electric aircraft design – a case study. MSc. Thesis, Technical University of Delft.

[3] Abolmoali, P., A. Donovan, S.S. Patnaik, P. McCarthy, D. Dierker, N. Jones, and R. Buettner. 2020. Integrated propulsive and thermal management system design for optimal hybrid electric aircraft performance. AIAA paper 2020-3557.

[4] https://www.onera.fr/en/news/how-can-we-reduce-fuel-consumption%3F-dragon

[5] Novelli, P. August 2021. IMOTHEP: towards hybrid propulsion for commercial aviation – project overview. In: *AIAA Aviation Forum*.

[6] Schmollgruber, P., C. Döll, J. Hermetz, R. Liaboeuf, M. Ridel, I. Cafarelli, O. Atinault, C. François, and B. Paluch. January 2019. Multi-disciplinary exploration of DRAGON: an ONERA hybrid electric distributed propulsion concept. In: *AIAA SciTech 2019,* San Diego, CA.

[7] Mason, W.H. September 1989. 1976 Standard atmosphere subroutine, Mason's BASIC program, converted to FORTRAN. Department of aerospace and ocean engineering, Virginia Tech, Blacksburg, VA 24061.

[8] Kreith, F., and W.Z. Black. 1980. Basic heat transfer. Harper and Row, New York.

[9] Holman, J. 1986. Heat transfer, 6th edition. McGraw-Hill.

[10] Oates, G.C. 1984. Aerothermodynamics of gas turbine and rocket propulsion. AIAA education series, 2nd printing, AIAA, Inc., New York.

[11] El-Sayed, A.F. 2017. Aircraft propulsion and gas turbine engines. CRC Press.

[12] Saravanamuttoo, H.I.H., H. Cohen, and G.F.C. Rogers. 2001. Gas turbine theory, 5th edition. Pearson.

[13] Moir, I., and A. Seabridge. 2008. Aircraft systems – mechanical, electrical and avionics subsystems integration. Third edition, John Wiley and Sons.

[14] Fanger, P.O. 1972. Thermal comfort – analysis and applications in environmental engineering. McGraw-Hill.

[15] International Organization for Standardization. 2005. Ergonomics of the thermal environment, analytical determination and interpretation of thermal comfort using calculation of the PMV and PPD indices and local thermal comfort criteria. ISO 7730, 3rd edition.

[16] Stolwijk, J.J. 1970. Mathematical model of thermoregulation. Chapter 48, Physiological and behavioral temperature regulation. Editors Hardy, Gagge and Stolwijk, Thomas.

[17] Tanabe, S., K. Kobayashi, J. Nakano, Y. Ozeki, and M. Konishi. 2002. Evaluation of thermal comfort using combined multi-node thermoregulation (65MN) and radiation models and computational fluid dynamics (CFD). *Energy and Buildings*, 34:637-646.

[18] Fiala, D. June 1998. Dynamic simulation of human heat transfer and thermal comfort. PhD Thesis. De Montfort University, Leicester, UK.

[19] Ahlers, M.F. 2020. An introduction to aircraft thermal management. SAE International.

[20] Wolff, M. 2011. Aerothermal design of an engine/vehicle thermal management system. RTO-EN-AVT-195.